International Journal of Nanomedicine

Dovepress
open access to scientific and medical research

Open Access Full Text Article

ORIGINAL RESEARCH

Combining nano-physical and computational investigations to understand the nature of "aging" in dermal collagen

Tarek Ahmed[1]
Anthony Nash[2]
Kristina EN Clark[3]
Marion Ghibaudo[4]
Nora H de Leeuw[2]
Anne Potter[4]
Richard Stratton[3]
Helen L Birch[5]
Ramona Enea Casse[4]
Laurent Bozec[1]

[1]Division of Biomaterials and Tissue Engineering, Eastman Dental Institute, University College London, [2]Department of Chemistry, University College London, [3]Centre for Rheumatology and Connective Tissue Diseases, Division of Medicine, University College London, London, UK; [4]L'Oréal Research and Innovation, Aulnay-sous-Bois, France; [5]Division of Surgery and Interventional Science, UCL Institute of Orthopaedics and Musculoskeletal Science, University College London, London, UK

Correspondence: Tarek Ahmed
Division of Biomaterials and Tissue Engineering, UCL Eastman Dental Institute, University College London, 256 Gray's Inn Road, London WC1X 8LD, UK
Tel +44 020 3456 1096
Email tarek.ahmed.10@ucl.ac.uk

Abstract: The extracellular matrix of the dermis is a complex, dynamic system with the various dermal components undergoing individual physiologic changes as we age. Age-related changes in the physical properties of collagen were investigated in particular by measuring the effect of aging, most likely due to the accumulation of advanced glycation end product (AGE) cross-links, on the nanomechanical properties of the collagen fibril using atomic force microscope nano-indentation. An age-related decrease in the Young's modulus of the transverse fibril was observed (from 8.11 to 4.19 GPa in young to old volunteers, respectively, $P<0.001$). It is proposed that this is due to a change in the fibril density caused by age-related differences in water retention within the fibrils. The new collagen–water interaction mechanism was verified by electronic structure calculations, showing it to be energetically feasible.

Keywords: collagen, aging, atomic force microscopy, nanomechanics, advanced glycation end products, nanotechnology

Introduction

Understanding how the human body ages is complex but timely, as the proportion of older population increases. In a recent report by the UK House of Lords,[1] it was suggested that children born after 2010 have life expectancies of 96 and 93 years (for girls and boys, respectively).[2] It is, therefore, essential to understand the nature and impact of the aging process on organs, as physiologic and functional characteristics of these organs change dramatically. Age-related changes have a deleterious impact on the structure and functions of the skin (protection, regulation and sensation).

Although changes can be observed directly at the surface of the skin, their sources arise at a molecular level. The skin dermal component is composed mostly of type-I collagen, secreted by dermal fibroblasts. The dermis is 2–3 mm thick, making up most of the thickness of our skin (80% of which is composed of type-I collagen).[3] It is composed of two layers: the papillary dermis (a thin network mesh of type-III collagen) and reticular dermis (thick bundles of collagen type-I fibers). These undergo different age-related changes.[4] Other major components of the dermal extracellular matrix (ECM) include elastic fibers (elastin), which provide mechanical elasticity allowing responsiveness to physical loading;[3,5] proteoglycans, decorin and versican, with a protein core and sulfated glycosaminoglycan (GAG) chains which are highly hydrophilic and provide water retention properties to the ECM;[6] and hyaluronic acid (HLA), a nonsulfated GAG chain which, due to its hydrophilicity, also has a great capacity to bind with water, providing hydration and water transport to the dermis.[7,8]

submit your manuscript | www.dovepress.com
Dovepress
http://dx.doi.org/10.2147/IJN.S121400

Dermal aging is a complex process with a number of changes occurring to the noncollagenous components of the dermal ECM (Figure 1). Elastin content declines as it is produced less,[5] and calcification of elastin fibers occurs, causing a deterioration in functional properties.[5] With elastin turnover approaching a lifespan, structural and physiochemical changes to the elastin network accumulate with age.[9,10] Decorin and versican undergo changes in their GAG chains, with studies showing a reduction in the molecular size of their polysaccharide chains.[6,11] HLA content in the dermis decreases as it is produced less by fibroblasts and disappears altogether in the epidermis as a function of age.[12] HLA synthesized in the dermis also sees a decrease in the size of the GAG chain.[3]

Both collagen and elastin undergo enzymatic and nonenzymatic cross-links in the ECM as a function of aging[13,14] (Figure 2). Lysyl oxidase (LOX) is an enzyme found in the ECM, in fibroblasts in the dermis and keratinocytes in the epidermis.[15] Following cleavage of collagen N-telopeptide and self-assembly of collagen molecules into fibrils, lysine and hydroxylysine residues undergo conversion into reactive aldehydes which react with other aldehydes or amine groups to form immature cross-links, eventually involving further amino acids to form mature covalent cross-links such as pyridinoline.[13] LOX maintains collagen alignment and fibril structure[16] and is crucial for maintaining homeostasis of elastin, with cross-linking preventing excessive elasticity of fibers as well as aiding deposition.[17] LOX activity is higher in skin than in other tissues,[18] showing an increase in expression in aged skin.[10] However, the proportion of LOX-derived cross-links compared to other covalent cross-links in the ECM reduces with age.[19] The proportion of nonenzymatic (glycation) cross-links, investigated in this study, increases, and therefore, they are associated with aging rather than the enzymatic LOX-derived cross-links.

Upon secretion of collagen into the dermal ECM for assembly into supramolecular structures, collagen can undergo an irreversible nonenzymatic glycation reaction, known as the Maillard reaction. During this glycation process, aldehyde groups from sugars react with amine functional groups found

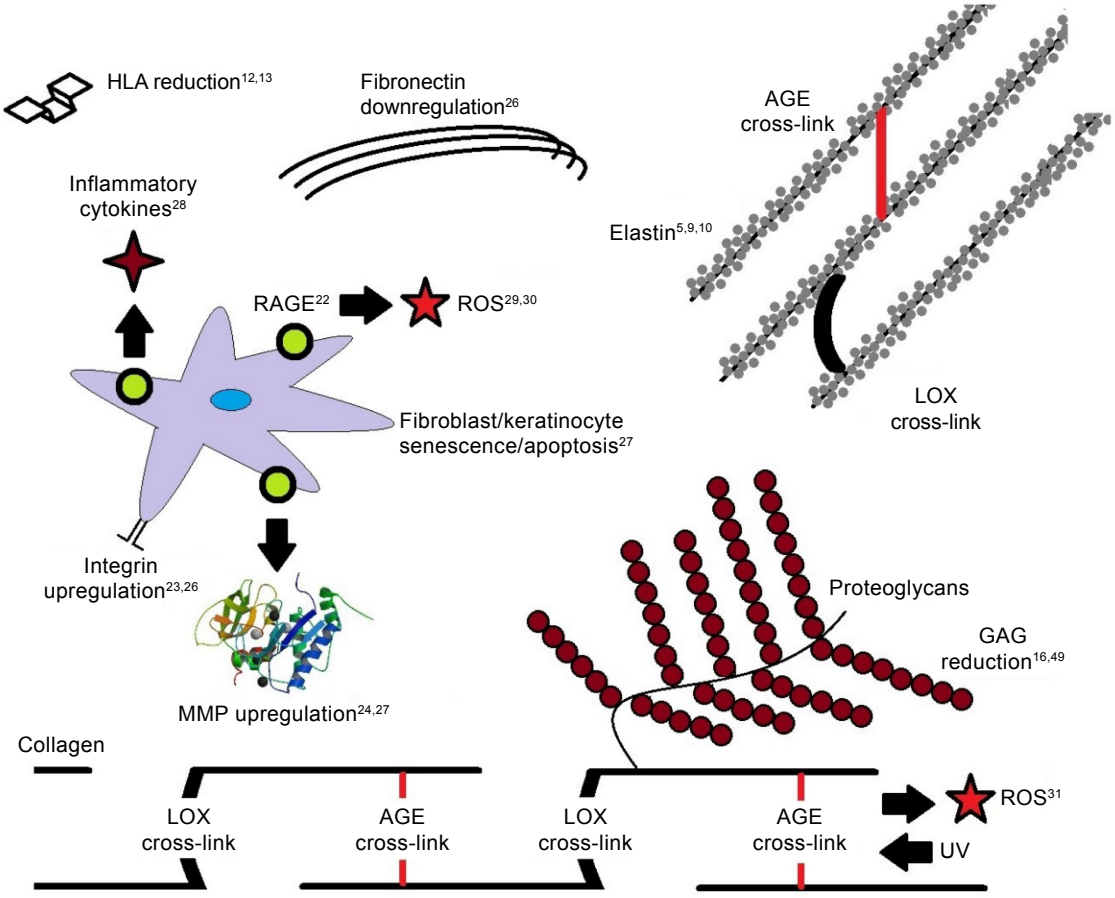

Figure 1 Age-related changes to components found within the dermal/epidermal ECM due to intrinsic and extrinsic aging processes.
Abbreviations: AGE, advanced glycation end product; ECM, extracellular matrix; GAG, glycosaminoglycan; HLA, hyaluronic acid; LOX, lysyl oxidase; MMP, matrix metalloproteinase; RAGE, receptor for advanced glycation end products; ROS, reactive oxygen species; UV, ultraviolet.

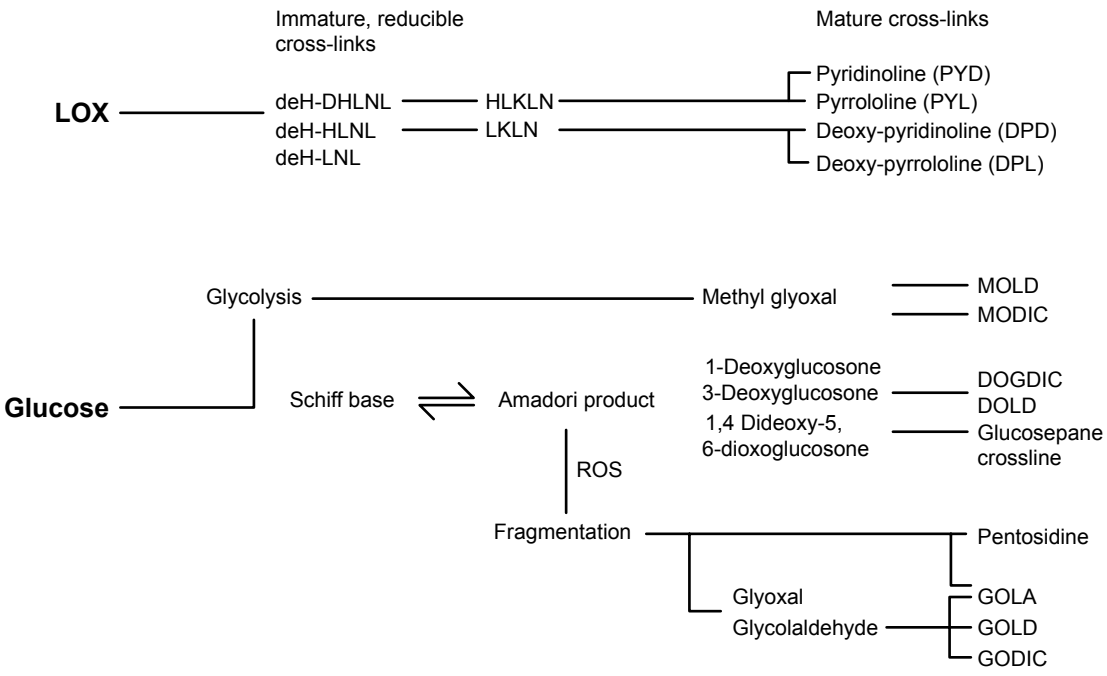

Figure 2 Products formed from for enzymatic and nonenzymatic covalent cross-linking of collagen.
Note: Data from Saito et al[13] and Monnier.[14]
Abbreviations: LOX, lysyl oxidase; ROS, reactive oxygen species; GOLA, glyoxal lysine amide; GODIC, glyoxal imidazolimine cross-link; GOLD, glyoxal lysine dimer; DOLD, deoxyglucosone lysine dimer; MOLD, methylglyoxal lysine dimer; DOGDIC, deoxyglucosone imidazolium cross-link; MODIC, methylglyoxal imidazonlimine cross-link; HLNL, hydroxylysinonorleucine; DHLNL, dihydroxylysinonorleucine; LNL, lysinonorleucine; LKLN, lysino-5-ketonorleucine; HLKLN, hydroxylysino-5-kenonorleucine.

on the collagen side chains. Further oxidation occurs and advanced glycation end products (AGEs) accumulate within the collagen matrix.[20] Both the rate of collagen turnover and the concentration of blood glucose are factors affecting the degree of accumulation,[19] with some AGEs producing covalent cross-links between the collagen residues.[21] Accumulation of AGEs due to intrinsic aging has been observed in the human skin by immunostaining of histology sections.[5]

Glucosepane is the most common AGE cross-link (between lysine and arginine) resulting from interaction of the collagen molecule with glucose, the highest concentrated sugar found in vivo.[22] Glucose exists mostly in its less-reactive closed chain form. Its more reactive open chain form only composes 0.002% of glucose molecules in vivo; therefore, significant collagen cross-linking requires a prolonged exposure to glucose.[23] A number of other AGE cross-links can also form, such as pentosidine,[24] DOGDIC (deoxyglucosone lysine–arginine cross-link), MOLD (methylglyoxal lysine dimer) and GOLD (glyoxal lysine dimer),[17,21] among others (Figure 2). Deoxyglucosone and glyoxal are formed due to fragmentation of the Amadori product (an intermediate precursor product to an AGE in the Maillard reaction) and are highly reactive, although they are found in very small concentrations in vivo.[17]

AGE accumulation affects other components of the ECM (Figure 1), including dermal and epidermal homeostasis.[25] First, cell activity can be drastically altered as glycation products bind to the receptor for advanced glycation end products (RAGE), triggering fibroblast and keratinocyte apoptosis through binding of (carboxymethyl)-lysine to RAGE[21] and senescence.[26] Cell signaling is also affected with the release of pro-inflammatory and profibrotic cytokines.[27] Second, AGE binding to cells can lead to production of reactive oxygen species, which can lead to acceleration of further AGE production.[28,29] When coupled with exposure to ultraviolet radiation (extrinsic aging, brought upon by environmental conditions), AGEs such as pentosidine can act as photosensitizers, accelerating oxidative damage, resulting in increased damage in older skin.[30] Third, synthesis of ECM components is also affected by RAGE binding, with the gene expression of matrix metalloproteinases and integrin being upregulated[22,25] and that of fibronectin being downregulated.[25] Synthesis of various collagen chains is affected,[25] and glycation of collagen can have a number of effects on its functional properties, increasing its resistance to digestion by enzymes.[28,31]

In this study, we aim to investigate the impact of age-dependent increased AGE accumulation on the collagen mechanical properties using both a nano-histology approach combined with computational analysis to test the hypotheses. This combined approach brings new insights into the intimate relationship between AGE accumulation, collagen fibril

mechanical properties and the role of water within collagen fibrils. This study hypothesizes changes in the nanoscale mechanical properties of collagen fibrils as a function of aging and will explore the potential mechanisms surrounding these changes.

Methods

Punch skin biopsies were collected from volunteers of Caucasian ethnicity with no known health conditions and of age <30 years (young group, n=3) or older than 60 years (old group, n=4). The young group consisted of one female and two males and had a mean age of 25.0±2.94 (standard deviation [SD]). The old group consisted of four females and had a mean age of 73.5±8.44 (SD). Ethical approval for this project was granted by the National Research Ethics Service (NRES) Committee London-Hampstead, Health Research Authority, Research Ethics Committee London Centre, REC ref 6398, and written informed consent was obtained from volunteers. Tissue was collected and stored in accordance with the code of practice from the Human Tissue Authority.

Punch biopsies (4 mm) were taken from the anterior forearm skin (less exposed to sunlight) of the volunteers and immediately snapped frozen by immersion in isopentane. Biopsies were embedded in cryo-embedding medium (Cryo-m-bed; Bright Instrument Company LTD, Luton, UK) and sectioned to 8 μm using a cryo-microtome. Tissue sections were physisorbed onto glass slides and stained using either Hematoxylin and Eosin or Pico Sirius Red. The samples were then stored at 4°C until experimentation.

Nanohistology and nanomechanics

Atomic force microscopy (AFM) imaging (XE-100; Park Systems, Seoul, South Korea and Nanowizard II; JPK Instruments, Berlin, Germany) was performed in contact mode using NP-S10 probes (Bruker, Santa Barbara, CA, USA) with a spring constant of 0.3 N m^{-1} at a scanning rate of 1.0 Hz or above. All AFM images were acquired directly from the histologic sections without any further processing or rehydration. Four sections were taken from each volunteer biopsy and a series of AFM images captured at four locations in the reticular dermis with scan sizes of 5×5, 10×10 and 40×40 μm^2. Scanning electron microscopy (SEM; XL-30 FEG SEM; FEI, Eindhoven, the Netherlands) was performed on sections coated with Au/Pd, using an acceleration voltage of 5 kV. Nanomechanical analysis was performed using a Nanowizard II AFM (JPK Instruments) system mounted on an Olympus IX71 (Olympus Corporation, Tokyo, Japan) inverted microscope. All AFM mechanical measurements were acquired directly on the histologic sections without any further processing or rehydration. All force–distance curves were acquired using RFESPA probes (Bruker) with a spring constant k=3 N m^{-1} used to indent radially individual collagen fibrils. All forces curves were then analyzed using a custom Matlab® algorithm, following the Oliver–Pharr modeling method to calculate the Young's modulus (E) for fibrils.[30]

Statistical analysis

Young's modulus of fibrils from the volunteers was compared using two-sided hypothesis testing with a significance level α=0.001. For unpaired comparison of young and old volunteer groups, two-tailed Student's *t*-test was used (Statistical Package for the Social Sciences 22) with an *F*-test to check for equality of variance. For comparison of volunteers within the young and old volunteer groups, one-way analysis of variance was used (Statistical Package for the Social Sciences 22).

Computational study

Computational geometry optimization of glucosepane water complexes was performed on an initial starting geometry taken from the final frame of a 60 ns explicitly solvated all-atom Molecular Dynamics simulation from a previous study.[32] Electronic structure calculations were performed using GAUSSIAN-98.[33] Using the integral equation formalism polarizable continuum model, all structure optimizations were performed in an implicit water solvent model. The modern density function theory (DFT) hybrid meta-generalized gradient approximation wb97xd functional, which contains empirical dispersion terms and long-range corrections, was used for all electronic structure optimizations and energy calculations in conjunction with the 6-311++g (2df,2p) basis set. Tight convergence criteria were adopted throughout, along with an ultrafine integration grid. Vibrational frequency analysis was performed for each optimized structure to verify that an energy minimum had been found. We used a zero-point corrected relative interaction energy value as a measure of hydrogen bond strength using the wb97xd functional. This was followed by a single-point energy calculation using the Møller–Plesset, MP2, post Hartree–Fock ab initio functional with the basis set aug-cc-pVDZ (correlation consistent double-zeta augmented with diffusion functions). Efforts were made to include a triple-zeta basis set, but due to the system size, this was not possible. To enable a fair comparison between DFT and ab initio interaction energies, the MP2 total system energy was

adjusted using the zero-point energy from the comparable DFT frequency calculation. The relative interaction energy, ΔE_{rel}, was calculated using the equation:

$$\Delta E_{rel} = \Delta E_{comp} - (\Delta E_{H_2O} + \Delta E_{AGE}),$$

where ΔE_{comp} is the total energy of the glucosepane–water complex, ΔE_{H_2O} is the total energy of the water molecule in isolation and ΔE_{AGE} is the total energy of glucosepane in isolation.

Results

Impact of aging on dermal collagen ultrastructure

Age-related changes in the structure of skin samples were investigated through a transverse section of the dermal layer. Figure 3 shows the optical images obtained from stained histologic sections of young, that is, 28-year-old volunteers (Figure 3A and B), and old, that is, 82-year-old volunteers (Figure 3C and D). Differences in dermis ultrastructure were observed using a standard light microscope (20× objective). Images in Figure 3A and C obtained from the Hematoxylin and Eosin-stained samples showed significant variation in the epidermis layer thickness (darker pink layer) in the older volunteer, whereas this remained homogenous in the younger volunteer. The biggest structural difference was observed in the Pico Sirius Red-stained sections. The overall ultrastructure of the collagen scaffold within the dermis varied considerably; older dermis appeared porous with large gaps intercalated between collagen-stratified layers, while younger dermis was denser, though discrete large gaps were found within the section.

To investigate the impact of aging on the quaternary structure of dermal collagen, both AFM and SEM imaging were carried out in the reticular region of the dermis. Figure 4A–D shows the representative images illustrating the ultrastructure of collagen scaffold found in the reticular dermis of the younger volunteer (28 years old). Figure 4A and B shows the SEM images of dense collagen sheets present in that region. The presence of cracks in Figure 4A is due to the vacuum-related desiccation and is an imaging artifact. However, highly ordered collagen fibrillar structure was observed in the cross-section of this histologic section (Figure 4B). Figure 4C shows highly contrasted D-banding periodicity, the fingerprint for collagen quaternary structure. Figure 4D shows the intersection of two dense collagen planes, showing that dense, banded collagen is also present deep within the dermal matrix. Overall, the ultrastructure of the collagen scaffold from younger volunteers can be summarized as a dense, compact scaffold with highly contrasted D-banding periodicity.

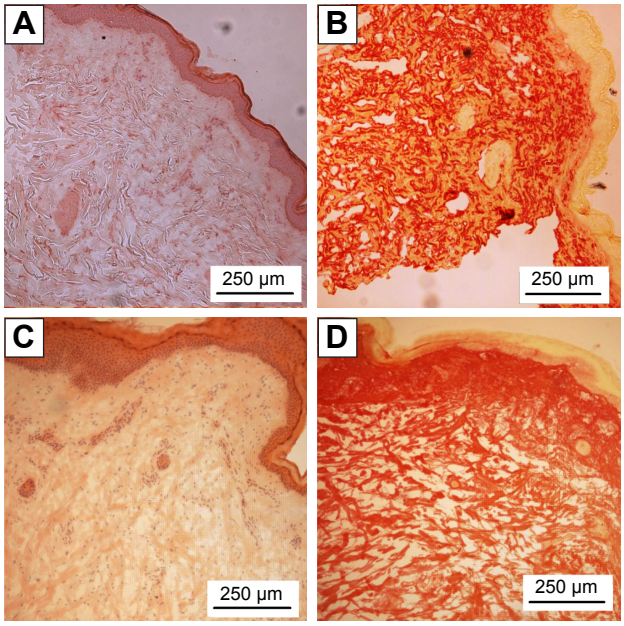

Figure 3 Histology sections stained in hematoxylin and eosin (**A**, **C**) and Pico Sirius Red (**B**, **D**) for a 28-year-old (**A**, **B**) and an 82-year-old volunteer (**C**, **D**), respectively.

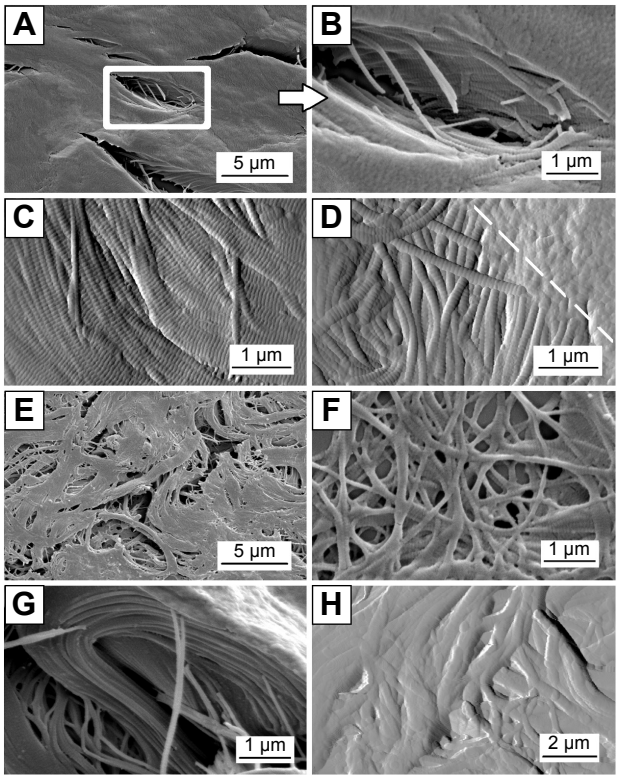

Figure 4 SEM images of volunteers aged <32 years (**A**, **B**). AFM images of volunteers aged <32 years (**C**, **D**). SEM images of volunteers aged >60 years (**E**–**G**). AFM image of volunteers aged >60 years (**H**).
Abbreviations: AFM, atomic force microscopy; SEM, scanning electron microscopy.

Collagen ultrastructure of older tissue sections varied significantly. Figure 4E–H shows the representative images presenting collagen scaffold found in the reticular dermis of an older volunteer (82 years old). Figure 4E is an SEM image of the collagen ultrastructure present in the reticular dermis. Fibrillar structure was fragmented with no overall cohesion; the scaffold was porous with a cluster of interstitial gaps appearing in between the fibril bundles. This is corroborated by Figure 4F taken by AFM in the same region, in which fibrils are randomly distributed and oriented. Figure 4G presents the remains of a large collagen sheet with fibril register and packing. Changes in the quaternary structure of collagen are exemplified in Figure 4H, which shows the collagen fibrils in a degraded state without the characteristic D-banding periodicity. Overall, the ultrastructure of the collagen scaffold from older volunteers can be summarized as a porous, fragmented scaffold with some loss of D-banding fibrillar periodicity.

Impact of aging on mechanical properties

Using AFM, it was possible to carry out systematic mechanical measurements directly on the histologic sections obtained from the seven volunteers. A series of localized force–distance curves were collected exclusively on the collagen fibrils, which is presented diagrammatically in Figure 5A. The measurement of collagen mechanical properties by AFM[34] has been shown to change depending on the level of fibrillar hydration.[35,36] To evaluate the impact of hydration on the mechanical properties of collagen, two sets of measurements were carried out on the same sections: first, in a dehydrated environment, followed by a repeat of the same measurements after 10 minutes rehydration in phosphate-buffered saline (PBS). The variation in fibrillar Young's modulus independent of age followed trends in the literature, which found a significant increase in fibril modulus upon dehydration.[36] In the case of hydrated fibrils, the mean hydrated fibril modulus of the young volunteer was $E_{y\text{-}hyd}$ = (1.24±0.09) MPa $N_{fibrils}$ =63 (Figure 5B) and for the old volunteer $E_{o\text{-}hyd}$ = (0.89±0.05) MPa $N_{fibrils}$ =64 (Figure 5C). In the case of air-dried, dehydrated fibrils, the mean fibril modulus for young volunteers was found to be $E_{y\text{-}dehyd}$ = (6.84±0.64) GPa $N_{fibrils}$ =128 (Figure 5D), and for old volunteers $E_{o\text{-}dehyd}$ = (4.03±0.38) GPa $N_{fibrils}$ =126

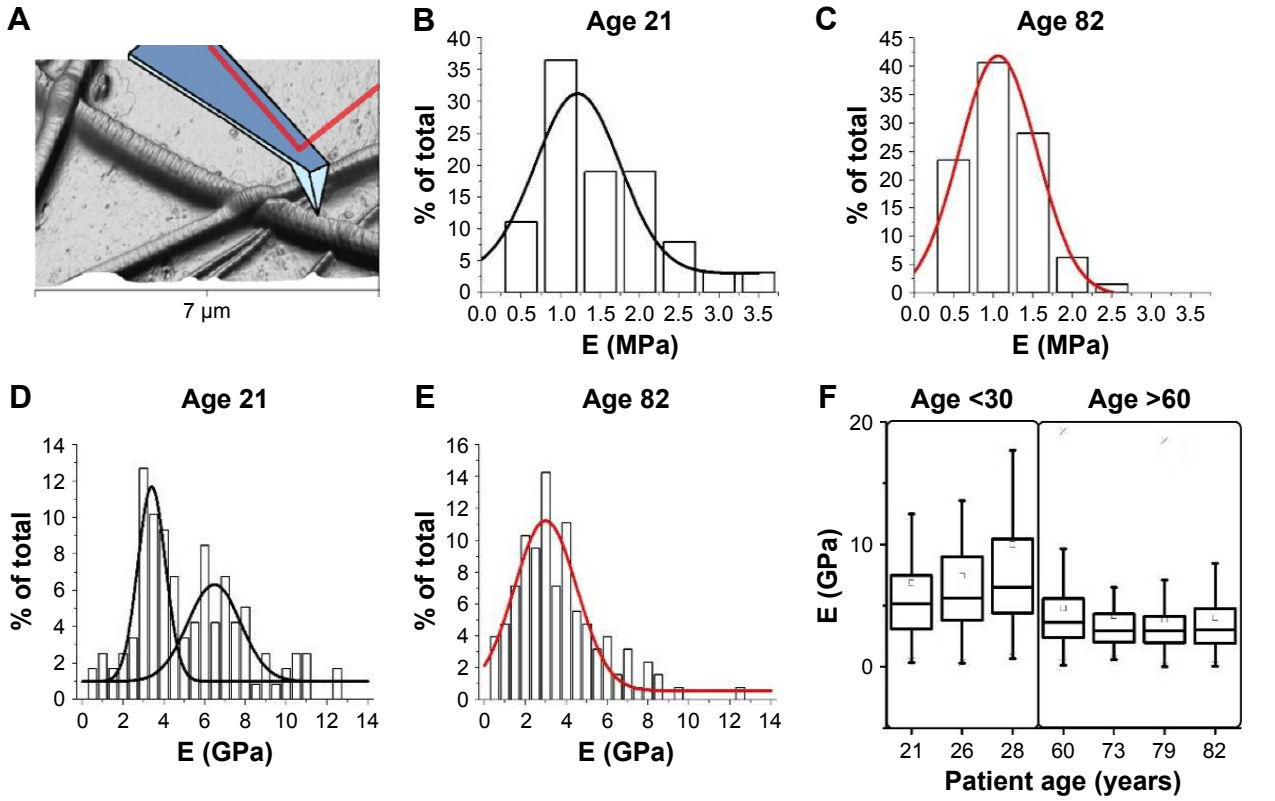

Figure 5 Nanoindentation of collagen fibrils.
Notes: Indentation of a fibril in radial direction (**A**). Distribution of Young's modulus for hydrated collagen fibrils for a young volunteer (**B**). Distribution of Young's modulus for hydrated collagen fibrils for an old volunteer (**C**). Distribution of Young's modulus for hydrated collagen fibrils for a young volunteer (**D**). Distribution of Young's modulus for dehydrated collagen fibrils for an old volunteer (**E**). Relationship between Young's modulus of dehydrated fibrils and age (**F**).
Abbreviation: E, Young's modulus.

(Figure 5E). As expected, there was a sharp increase in the stiffness of the collagen fibril as a result of sample dehydration. However, the values of moduli for both hydrated samples (young and old) did not fit the criteria for being significantly different, (P=0.001), shown in Figure 5B and C, whereas the values of moduli for both dehydrated samples (young and old) were significantly different, (P<0.001) and illustrated in Figure 5D and E. It was interesting to note that Figure 5D exhibited a bimodal distribution in Young's Modulus with the first mode centering on a mean $E_{y.dehyd.mode.1}$ =3.31 GPa, similar to the older volunteer's mean Young's Modulus. A second mode is observed centring on a mean $E_{y.dehyd.mode.2}$ =5.70 GPa. Experimentally, rehydration of the histological sections had a significant impact on stability of the sample, as over 9/10 of histological sections desorbed from their original cover slide upon rehydration. As a result of the high rate of desorption of the section, it was decided to perform all the measurements on air-dried sections and explore whether the transverse Young's Modulus values were independent of volunteer age. AFM-based nano-indentation was carried out on air-dried sections from all 7 volunteers and the transverse Young's Modulus was plotted as function of the volunteers' age as shown in Figure 5F. The mean Young's Modulus for young volunteers was E_y= (8.11±0.46) GPa, $N_{fibrils}$ =362 and the mean Young's Modulus for older volunteers was E_o= (4.19±0.21) GPa, $N_{fibrils}$ =477 showing a statistically significant reduction in Young's modulus with age (P<0.001). The variance of the Young's Modulus was also found to decrease for older volunteers (σ_y^2=65.77 GPa, σ_o^2=17.56 GPa). There were no significant differences found between volunteers within each cohort, young or old (P>0.001).

Deciphering glucosepane–water interaction by computational methodology

Nanomechanical measurements suggested a possible change in fibril hydration, so a computational approach was deployed to investigate favorable water-binding sites at the atomistic glucosepane structure. An all-atom structure of glucosepane proposed by Biemel et al[37] was extracted from the final frame of an earlier Molecular Dynamics study.[32] The backbone atoms were removed and a methyl group terminated the α-carbon atom on both aliphatic chains. This procedure reduced the computational expense and ensured the isolation of an explicit water molecule to the polar binding regions of the glucosepane compound rather than the polypeptide backbone. An explicit water molecule was manually positioned 1.8 Å from each polar site. As per the visual depiction of the final optimized structures (Figure 6), a water molecule was orientated to act as an electron acceptor to each nitrogen in the imidazole group, resulting in structures I and II, as an electron donor to each hydroxyl group, resulting in structures III and IV, and as an electron acceptor to each hydroxyl group to form structures V and VI. Electronic structure optimization of single water-bound glucosepane hydrates, unbound glucosepane and a single water molecule was performed using the wb97xd functional with a 6-311++g(2df,2p) basis set

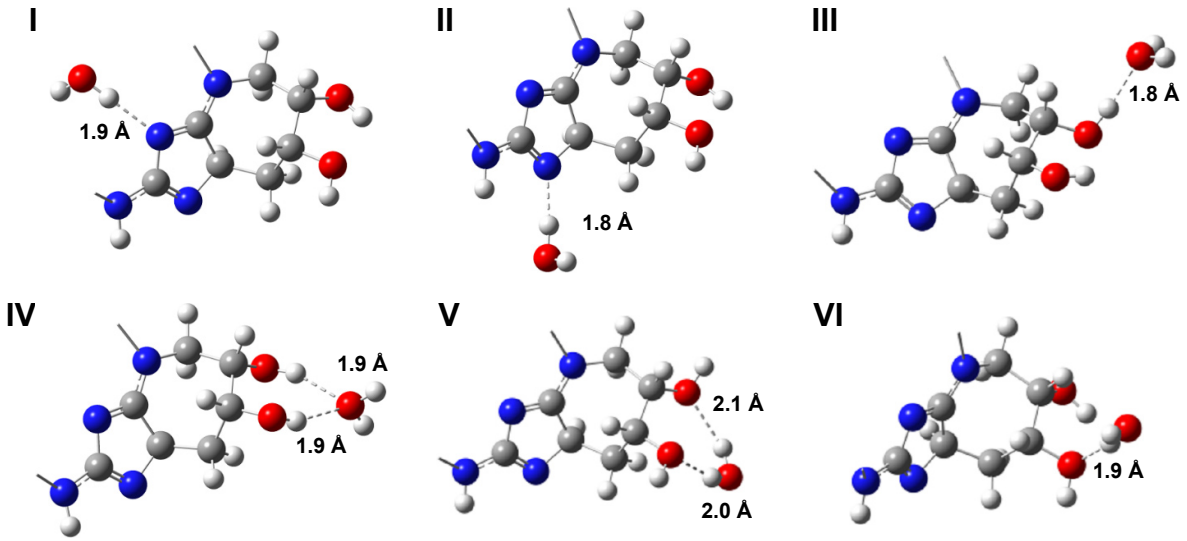

Figure 6 I–VI show various optimized electronic structure calculations of glucosepane in coordination with a single water molecule. Intermolecular distance between the hydrogen bond acceptors and donors are labeled appropriately. Aliphatic side chain tails have been removed for clarity.

to a tight convergence on an ultrafine integration grid in an implicit water solvent. Optimized structures are presented in Figure 6, and relative interaction energies are presented in Table 1, all of which present a stable and energetically favorable interaction between water and glucosepane. MP2 single point entry (SPE) calculations using the aug-cc-pVDZ basis set and corrected using the zero point energy (ZPE) value from the DFT frequency calculations complement the trend in the DFT energy calculations. All ZPE calculations were approximately 308 kcal mol^{-1}.

The interaction between an electron donor molecule with a strong polar group, OH, typically results in a change in O–H bond length, denoted by Δd(O–H). In addition, these interactions are usually identified with distances between 1.3 and 2.3 Å. The optimized coordination of water to the nitrogen presented in structure I resulted in a Δd(O–H) of 0.01931 Å and presented an intermolecular distance of 1.8835 Å. Upon coordinating water with the opposite nitrogen, structure II, we noted a decrease in the intermolecular distance by 0.1086 Å when compared with the intermolecular distance observed in structure I and a Δd(O–H) of 0.02903 Å. The greater distance between the hydroxyl group in question in structure II from the lysine nitrogen results in an increase in electronegativity on the hydroxyl oxygen, thus promoting further stability by as much as 1.4031 and 0.3397 kcal mol^{-1} according to DFT and ab initio calculations, respectively.

The optimized structure of an energetically favorable coordination of a single water electron acceptor, 1.7977 Å from the hydroxyl group, can be seen in structure III. Attempts at the mono-coordination of the second hydroxyl group resulted in a single water molecule acting as an electron acceptor to both hydroxyl group donors (seen in structure IV), due in part to the inherent orientation of one hydroxyl group to the neighboring hydroxyl group resulting in an intramolecular noncovalent interaction. A similar network of noncovalent intramolecular interactions has been observed in glucose derivatives.[38] With the electronegativity of the oxygen shared between both electron donors, the intermolecular distance was increased to 1.9120 and 1.9475 Å. In addition, neither hydroxyl group experiences a significant O–H bond stretch, reporting a Δd(O–H) of only 0.00732 and 0.00708 Å, respectively. Yet, the paired intermolecular coordination resulted in a significantly more stable structure.

Coordinating water as an electron donor to the lone pairs on the hydroxyl group resulted in a single intermolecular association, structure VI, and a dual intermolecular association, structure V. The structures demonstrated Δd(O–H) of 0.00403, 0.00848 and 0.01022 Å, respectively, while reporting intermolecular distances within expected hydrogen bond cutoffs. Furthermore, each structure yielded relative interaction energies indicative of a stable water association. Compared with the single association between water and glucosepane in structure VI, structure V pertains to a stable conformation from an additional bond resulting in a decrease in relative interaction energy by 0.8289 and 0.1778 kcal mol^{-1}, according to DFT and ab initio calculations, respectively.

Table 1 Relative interaction energies (kcal mol^{-1}) derived from optimized electronic structure calculations

Name	ΔE_{rel} (wb97xd)	ZPE (wb97xd)	ΔE_{rel} (MP2)
I	–5.3269	308.94	–6.5946
II	–6.7300	308.59	–6.9343
III	–3.9414	308.65	–4.6669
IV	–5.8710	308.69	–6.5539
V	–4.1610	308.47	–4.4244
VI	–3.3321	308.94	–4.2465

Notes: Energies calculated using the wb97xd functional were corrected using a zero-point energy correction value obtained from vibrational frequency analysis. MP2 ab initio calculations were derived from single-point energy calculations and corrected using the zero-point energy of the DFT frequency calculation.

Discussion

The porosity or fragmentation of the dermis observed in stained histology sections has been reported previously in a study involving volunteers (aged 2–85 years with 121 skin samples).[39] Bonta et al reported changes in the morphology of collagen fibers in volunteers over the age of 50, including fragmentation and disorganization of thick collagen fibers, lysis of thin fibers and an overall decrease in matrix density.[39]

The changes in quaternary structure observed in this study through SEM and AFM imaging showed an age-related decrease in collagen matrix density and loss of homogeneity of fibers. This supports earlier reports of changes at the macroscale[40] as well as a previous AFM study reporting nanoscale morphologic changes with age. In Fenske and Lober's study, collagen fibrils in young skin (age 21) were also found to be tightly packed and aligned in comparison to sparse, fragmented and disorganized fibrils in old skin (age 55).[41]

The lack of statistically significant difference in Young's modulus of hydrated fibrils between young and older volunteers suggests that transverse moduli for collagen in fully hydrated environments are not impacted by the age of volunteers. However, it is likely that complete rehydration is not physiologically relevant. As collagen fibrils become saturated with water, it leads to increases in fibril diameter.[42] There is little evidence that this water saturation happens

in vivo, therefore the results of the mechanical investigation of fully hydrated fibrils have to be considered carefully.

The age-related reduction in air-dried fibril stiffness is not consistent with earlier reports investigating the biomechanical properties of skin, which have overwhelmingly reported increases in stiffness.[26] A number of in vitro and ex vivo studies have investigated the mechanical properties of various tissues as a function of AGE accumulation due to both aging and diabetes (severe AGE accumulation occurs due to elevated blood glucose concentration[20]). An age-related stiffening of tissue was observed in tendon, vascular and myocardial tissue, cartilage and skin.[9,10,18,43] A stiffening of tissue was also observed in diabetic volunteers. A notable in vitro study reported an increase in stiffness of rabbit tendon incubated with glucose.[44] Ex vivo measurements of skin autofluorescence have shown that the concentration of AGEs in skin increases greatly with age,[9] with an age-dependent stiffening observed[26] supporting earlier reports.[45]

There were, however, a number of ex vivo studies looking at non-AGE-specific age-related changes in Achilles tendon[16] and gastrocnemius tendon,[25] which reported a decrease in stiffness with age. One report investigating the Young's modulus of dermal matrix for volunteers aged between 26 and 66 years (n=20) reported an increase in stiffness in the dermis for the 26–55 age group, followed by a reduction in stiffness for volunteers aged in their 60s, though this was not investigated or explained in further detail.[46] This study measured stiffness of hydrated samples, indenting with a 5 µm glass sphere mounted to a soft (k=0.02 N m^{-1}) cantilever. Thus, indentation of skin measured overall stiffness of the collagen matrix including other components of the skin (elastin, HLA and proteoglycans), and so, the macroscale mechanical properties of the bulk tissue rather than those of individual fibrils.

In this study, collagen fibrils were indented radially rather than longitudinally along the fibril axis. Thus, the Young's modulus obtained is the transverse modulus measuring indirectly the density of the fibril as it is compressed. The age-related reduction in transverse stiffness, therefore, relates to a change in the density of the fibril. Since all the samples were dehydrated passively in air, it is likely that any fibrillar interstitial water is no longer present. A previous study[42] performed dehydration experiments on model collagen scaffolds to evaluate the impact of one subset of cross-links (riboflavin mediated) and concluded that the collagen with cross-links retained water longer upon dehydration, when compared to non-cross-linked collagen, implying a cross-link-dependent collagen–water interaction. Taking this into consideration as well as the experimental data obtained, we proposed that the decrease in density of the collagen fibril with age is related to the level of water retained within the fibril. The presence of a bimodal distribution with a sharp peak at low Young's modulus complemented by a broad distribution of stiffer fibrils (Figure 5B) indicates the young volunteer has two distinct groups of fibrils, glycated and nonglycated, while the old volunteer has primarily one group of fibrils, glycated. However, to validate this hypothesis, it is necessary to understand the mechanisms by which collagen fibrils may retain water and whether this mechanism evolves as a function of aging.

Proposed relationship between stiffness and fibril hydration

The relationship between hydration and age-related changes in stiffness could be directly related to the accumulation of AGEs in dermal collagen. The hydrophilic properties of the AGE cross-links (such as glucosepane) play a central role in retaining the water molecules through interactions with the hydroxyl groups found on the AGE complex. It is at the nanoscale fibrillar level where water retention influences the stiffness of collagen. Three currently accepted forms of collagen hydration are shown in Figure 7A. Glucosepane is present in human tissues at levels 10–1,000 times higher than any other cross-linking AGE, and is currently considered to be the most important cross-linking AGE.[23] Glucosepane has two hydroxyl groups, leading to the possibility of water interaction due to its hydrophilic nature, as illustrated by Figure 7B. Therefore, as the volunteer ages and more glucosepane cross-links accumulate, more water molecules may be bound within the fibril as shown in Figure 7B. As water binds within the fibril, its density decreases, leading to a decrease in the radial stiffness of the fibril. The indentation process rather than compressing the collagen fibril directly begins probing the properties of water flow within the fibril (Figure 7C) before indentation of the fibril occurs. The overall indentation, therefore, is constituted by both a collagen fibril compression component and a water flow component, thus reducing the transverse Young's modulus. This hypothesis resides on an affinity between interstitial water present in the fibrils and AGE-mediated cross-links such as glucosepane.

Computational analysis of the glucosepane–water model suggests heterogeneous noncovalent interactions

A systemic approach of electronic structure optimization and single-point energy calculations of glucosepane within close proximity to a single water molecule helped identify stable

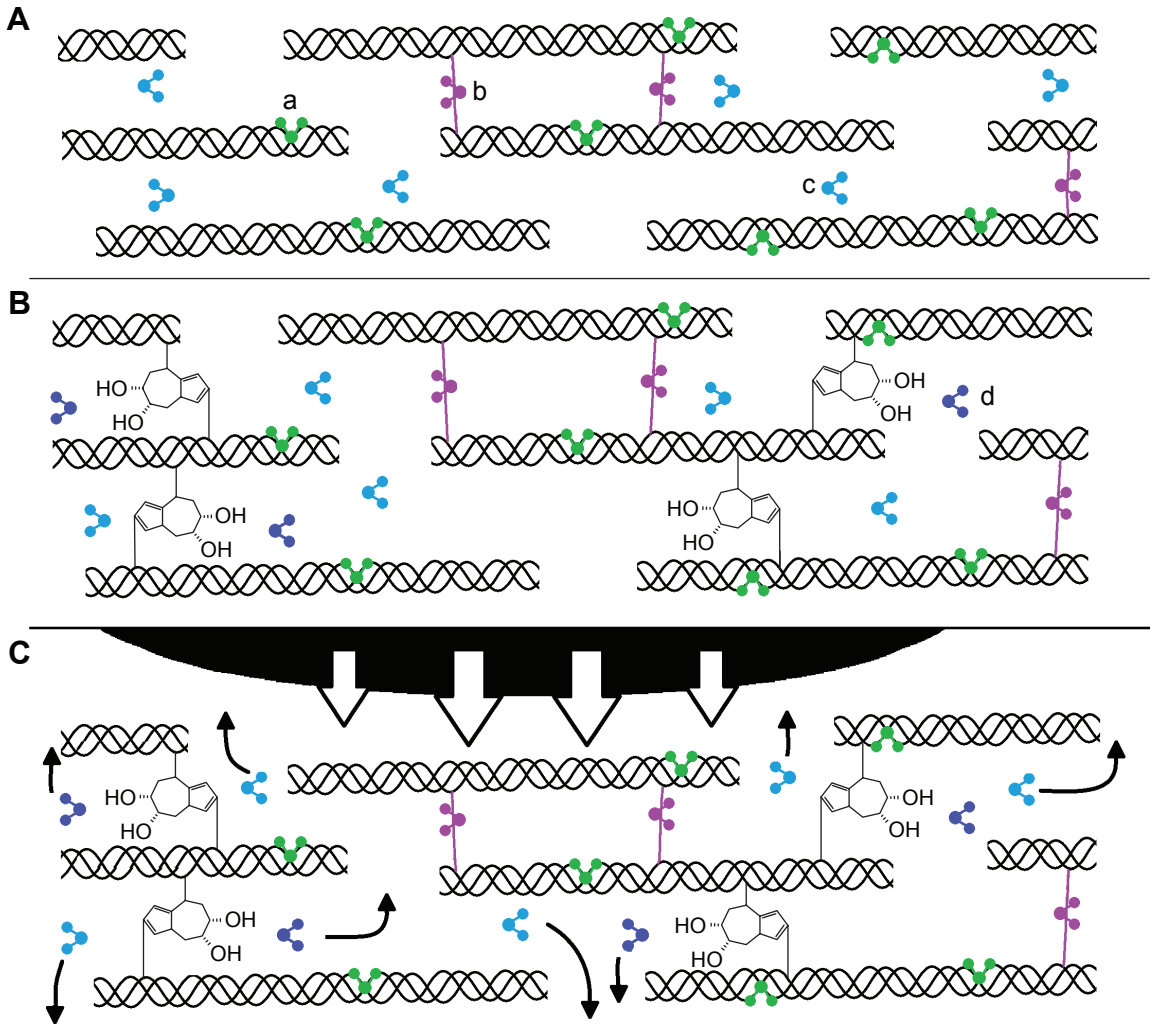

Figure 7 Illustrations for the three known modes of water interaction with collagen molecules: (**A**) covalently bonded to the molecule (a, green), water bridges between molecules (b, purple) and free-flowing water (c, blue). (**B**) The proposed mode of water interaction: water retention caused by glucosepane accumulation (d). (**C**) Proposed mechanism of water flow within the collagen fibril caused by nano-indentation.

single water molecule coordination. Although coordination of water as a hydrogen donor produced a stable conformation, stability through the coordination of the glucosepane hydroxyl groups as hydrogen donors resulted in lower relative interaction energy. In addition, coordination with the imidazole nitrogen furthest from the lysine side chain yielded the greatest decrease in interaction energy, resulting in the strongest identified hydrogen bond. Providing water can access glucosepane within the fibrillar environment; it will associate through a weak electrostatic attraction, which could potentially result in a region of ordered water around the AGE.

Increased collagen–water interaction, a response to aging?

The increased accumulation of AGE cross-links coincides with age-dependent changes of other major components of the dermis, primarily the reduction of GAG and HLA. The effect of GAG reduction is threefold; first, loss of the hydrophilic GAG chain reduces the water storage capacity within the dermis. Second, decorin GAGs bind to type-1 collagen, aiding fibrillogenesis and maintaining the fibril structure.[15,47] Third, decorin binding has been shown to inhibit cleavage of collagen by matrix metalloproteinase (the loss of decorin GAGs may result in increased enzymatic degradation of collagen fibrils,[42] leading indirectly to a change in the collagen matrix).

Conclusion

The loss of HLA and GAG chains from proteoglycans results in a significant age-related reduction of the capacity of the dermis to retain water, dramatically changing the mechanical properties of the ECM. This study suggests that the accumulation of AGE cross-links, which increase the interaction of water with collagen, could be a response to the loss of water retention capacity elsewhere in the dermal ECM.

This study is the first to identify using AFM unique nanoscale morphologic differences found in collagen fibril structure as a function of aging in skin. In addition, this study was the first to observe an age-dependent decrease in the transverse stiffness of collagen fibrils. A proposed water retention mechanism was verified by electronic structure calculations showing single water molecule association in an implicit solvent to be energetically stable. It is proposed that the properties of collagen in skin are responsive to adapt to changes in other major components of dermal ECM to preserve its functional properties. Further studies are required to characterize water retention using other techniques, as well as investigate this phenomenon in other collagenous tissues.

As discussed earlier, there are multiple processes that the various components of the dermis undergo during aging. This study focused specifically on changes occurring in collagen fibril morphology and mechanical properties from accumulation of AGE products. The impact, however, of the other age-dependent processes on the results in this study are not known.

Acknowledgments

The authors would like to thank first and foremost all the volunteers who kindly participated in this study. The authors would also like to thank Nicola Mordan for her advice and support for microscopy, Bruno Bernard, Hervé Pageon and Hélène Zucchi for their valuable advice about glycation, Jörg Sassmannshausen for his support with computational calculations and the Pathology core facility, Blizard Institute, Queen Mary, University of London for sample preparation of biopsy sections. This work was supported by L'Oreal and Biotechnology and Biological Sciences Research Council (BBSRC).

Disclosure

Helen L Birch received BBSRC grant BB/K007785/1 which supported this project. Anne Potter, Marion Ghibaudo, and Ramona Enea Casse are employees of L'Oréal. The authors report no other conflicts of interest in this work.

References

1. Select Committee on Public Service and Demographic Change Report of Session 2012–13 M. *Ready for Ageing?* London, UK: The Stationery Office Limited; 2013. Authority of the House of Lords; 5 March 2013. HL Paper 140.
2. ONS. *2010-based national population projections lifetable template*. England and Wales: Office of National Statistics; 2011.
3. Lovell CR, Smolenski KA, Duance VC, Light ND, Young S, Dyson M. Type I and III collagen content and fibre distribution in normal human skin during ageing. *Br J Dermatol*. 1987;117(4):419–428.
4. Mine S, Fortunel NO, Pageon H, Asselineau D. Aging alters functionally human dermal papillary fibroblasts but not reticular fibroblasts: a new view of skin morphogenesis and aging. *PLoS One*. 2008;3(12):e4066.
5. Jeanmaire C, Danoux L, Pauly G. Glycation during human dermal intrinsic and actinic ageing: an in vivo and in vitro model study. *Br J Dermatol*. 2001;145(1):10–18.
6. Carrino DA, Calabro A, Darr AB, et al. Age-related differences in human skin proteoglycans. *Glycobiology*. 2011;21(2):257–268.
7. Necas J, Bartosikova L, Brauner P, Kolar J. Hyaluronic acid (hyaluronan): a review. *Vet Med*. 2008;53(8):397–411.
8. Reiser KM, Hennessy SM, Last JA. Analysis of age-associated changes in collagen crosslinking in the skin and lung in monkeys and rats. *Biochim Biophys Acta*. 1987;926(3):339–348.
9. Shapiro SD, Endicott SK, Province MA, Pierce JA, Campbell EJ. Marked longevity of human lung parenchymal elastic fibers deduced from prevalence of D-aspartate and nuclear weapons-related radiocarbon. *J Clin Invest*. 1991;87(5):1828–1834.
10. Langton AK, Griffiths CE, Sherratt MJ, Watson RE. Cross-linking of structural proteins in ageing skin: an in situ assay for the detection of amine oxidase activity. *Biogerontology*. 2013;14(1):89–97.
11. Maquart FX, Brézillon S, Wegrowski Y. Proteoglycans in skin aging. In: Farage MA, Miller KW, Maibach HI, editors. *Textbook of Aging Skin*. Berlin, Heidelberg: Springer Berlin Heidelberg; 2010:109–120.
12. Kobayashi H, Ishii M, Chanoki M, et al. Immunohistochemical localization of lysyl oxidase in normal human skin. *Br J Dermatol*. 1994;131(3):325–330.
13. Saito M, Marumo K. Collagen cross-links as a determinant of bone quality: a possible explanation for bone fragility in aging, osteoporosis, and diabetes mellitus. *Osteoporos Int*. 2010;21(2):195–214.
14. Monnier VM, Mustata GT, Biemel KL, et al. Cross-linking of the extracellular matrix by the maillard reaction in aging and diabetes: an update on "a puzzle nearing resolution". *Ann N Y Acad Sci*. 2005;1043(1):533–544.
15. Chanoki M, Ishii M, Kobayashi H, et al. Increased expression of lysyl oxidase in skin with scleroderma. *Br J Dermatol*. 1995;133(5):710–715.
16. Bailey AJ. Molecular mechanisms of ageing in connective tissues. *Mech Ageing Dev*. 2001;122(7):735–755.
17. Liu X, Zhao Y, Gao J, et al. Elastic fiber homeostasis requires lysyl oxidase-like 1 protein. *Nat Genet*. 2004;36(2):178–182.
18. Kuivaniemi H. Partial characterization of lysyl oxidase from several human tissues. *Biochem J*. 1985;230(3):639–643.
19. Szauter KM, Cao T, Boyd CD, Csiszar K. Lysyl oxidase in development, aging and pathologies of the skin. *Pathol Biol (Paris)*. 2005;53(7):448–456.
20. Nass N, Bartling B, Navarrete Santos A, et al. Advanced glycation end products, diabetes and ageing. *Z Gerontol Geriatr*. 2007;40(5):349–356.
21. Alikhani Z, Alikhani M, Boyd CM, Nagao K, Trackman PC, Graves DT. Advanced glycation end products enhance expression of pro-apoptotic genes and stimulate fibroblast apoptosis through cytoplasmic and mitochondrial pathways. *J Biol Chem*. 2005;280(13):12087–12095.
22. Molinari J, Ruszova E, Velebny V, Robert L. Effect of advanced glycation endproducts on gene expression profiles of human dermal fibroblasts. *Biogerontology*. 2008;9(3):177–182.
23. Okano Y, Masaki H, Sakurai H. Dysfunction of dermal fibroblasts induced by advanced glycation end-products (AGEs) and the contribution of a nonspecific interaction with cell membrane and AGEs. *J Dermatol Sci*. 2002;29(3):171–180.
24. Aoki Y, Yazaki K, Shirotori K, et al. Stiffening of connective tissue in elderly diabetic patients: relevance to diabetic nephropathy and oxidative stress. *Diabetologia*. 1993;36(1):79–83.
25. Pageon H, Zucchi H, Dai Z, et al. Biological effects induced by specific advanced glycation end products in the reconstructed skin model of aging. *Biores Open Access*. 2015;4(1):54–64.
26. Ravelojaona V, Robert AM, Robert L. Expression of senescence-associated beta-galactosidase (SA-beta-Gal) by human skin fibroblasts, effect of advanced glycation end-products and fucose or rhamnose-rich polysaccharides. *Arch Gerontol Geriatr*. 2009;48(2):151–154.
27. Uchiki T, Weikel KA, Jiao W, et al. Glycation-altered proteolysis as a pathobiologic mechanism that links dietary glycemic index, aging, and age-related disease (in nondiabetics). *Aging Cell*. 2012;11(1):1–13.

28. Wondrak GT. Let the sun shine in: mechanisms and potential for therapeutics in skin photodamage. *Curr Opin Investig Drugs*. 2007; 8(5):390–400.
29. Wondrak GT, Roberts MJ, Jacobson MK, Jacobson EL. Photosensitized growth inhibition of cultured human skin cells: mechanism and suppression of oxidative stress from solar irradiation of glycated proteins. *J Invest Dermatol*. 2002;119(2):489–498.
30. Bastien PH. Aged human skin is more susceptible than young skin to accumulate advanced glycoxidation products induced by sun exposure. *J Aging Sci*. 2013;1:112.
31. DeGroot J, Verzijl N, Wenting-Van Wijk MJ, et al. Age-related decrease in susceptibility of human articular cartilage to matrix metalloproteinase-mediated degradation: the role of advanced glycation end products. *Arthritis Rheum*. 2001;44(11):2562–2571.
32. Collier TA, Nash A, Birch HL, de Leeuw NH. Preferential sites for intramolecular glucosepane cross-link formation in type I collagen: a thermodynamic study. *Matrix Biol*. 2015;48:78–88.
33. Gaussian Inc. 2009. *Gaussian 09* [computer program]. Wallingford, CT: Gaussian, Inc.; 2009.
34. Gutsmann T, Fantner GE, Kindt JH, Venturoni M, Danielsen S, Hansma PK. Force spectroscopy of collagen fibers to investigate their mechanical properties and structural organization. *Biophys J*. 2004;86(5): 3186–3193.
35. Grant CA, Brockwell DJ, Radford SE, Thomson NH. Effects of hydration on the mechanical response of individual collagen fibrils. *Appl Phys Lett*. 2008;92(23):233902.
36. Grant CA, Brockwell DJ, Radford SE, Thomson NH. Tuning the elastic modulus of hydrated collagen fibrils. *Biophys J*. 2009;97(11): 2985–2992.
37. Biemel KM, Friedl DA, Lederer MO. Identification and quantification of major maillard cross-links in human serum albumin and lens protein. Evidence for glucosepane as the dominant compound. *J Biol Chem*. 2002;277(28):24907–24915.
38. Silla JM, Cormanich RA, Rittner R, Freitas MP. Does intramolecular hydrogen bond play a key role in the stereochemistry of α- and β-d-glucose? *Carbohydr Res*. 2014;396:9–13.
39. Bonta M, Daina L, Muţiu G. The process of ageing reflected by histological changes in the skin. *Rom J Morphol Embryol*. 2013;54(Suppl 3): 797–804.
40. Fenske NA, Lober CW. Structural and functional changes of normal aging skin. *J Am Acad Dermatol*. 1986;15(4 Pt 1):571–585.
41. Quan T, Qin Z, Robichaud P, Voorhees JJ, Fisher GJ. CCN1 contributes to skin connective tissue aging by inducing age-associated secretory phenotype in human skin dermal fibroblasts. *J Cell Commun Signal*. 2011; 5(3):201–207.
42. Rich H, Odlyha M, Cheema U, Mudera V, Bozec L. Effects of photochemical riboflavin-mediated crosslinks on the physical properties of collagen constructs and fibrils. *J Mater Sci Mater Med*. 2014;25(1): 11–21.
43. Knott L, Bailey AJ. Collagen cross-links in mineralizing tissues: a review of their chemistry, function, and clinical relevance. *Bone*. 1998; 22(3):181–187.
44. Reddy GK. Glucose-mediated in vitro glycation modulates biomechanical integrity of the soft tissues but not hard tissues. *J Orthop Res*. 2003;21(4):738–743.
45. Bucala R, Cerami A. Advanced glycosylation: chemistry, biology, and implications for diabetes and aging. *Adv Pharmacol*. 1992;23:1–34.
46. Achterberg VF, Buscemi L, Diekmann H, et al. The nano-scale mechanical properties of the extracellular matrix regulate dermal fibroblast function. *J Invest Dermatol*. 2014;134(7):1862–1872.
47. Reese SP, Underwood CJ, Weiss JA. Effects of decorin proteoglycan on fibrillogenesis, ultrastructure, and mechanics of type I collagen gels. *Matrix Biol*. 2013;32(7–8):414–423.